PNAS RESEARCH ARTICLE | CELL BIOLOGY

A human FLII gene variant alters sarcomeric actin thin filament length and predisposes to cardiomyopathy

Yasuhide Kuwabara[a], Allen J. York[a], Suh-Chin Lin[a], Michelle A. Sargent[a], Kelly M. Grimes[a], James P. Pirruccello[b], and Jeffery D. Molkentin[c,1]

Edited by Jonathan Seidman, Harvard University, Boston, MA; received August 9, 2022; accepted April 7, 2023

To better understand the genetic basis of heart disease, we identified a variant in the *Flightless-I homolog* (*FLII*) gene that generates a R1243H missense change and predisposes to cardiac remodeling across multiple previous human genome-wide association studies (GWAS). Since this gene is of unknown function in the mammalian heart we generated gain- and loss-of-function genetically altered mice, as well as knock-in mice with the syntenic R1245H amino acid substitution, which showed that Flii protein binds the sarcomeric actin thin filament and influences its length. Deletion of *Flii* from the heart, or mice with the R1245H amino acid substitution, show cardiomyopathy due to shortening of the actin thin filaments. Mechanistically, Flii is a known actin binding protein that we show associates with tropomodulin-1 (TMOD1) to regulate sarcomere thin filament length. Indeed, overexpression of leiomodin-2 in the heart, which lengthens the actin-containing thin filaments, partially rescued disease due to heart-specific deletion of *Flii*. Collectively, the identified *FLII* human variant likely increases cardiomyopathy risk through an alteration in sarcomere structure and associated contractile dynamics, like other sarcomere gene-based familial cardiomyopathies.

heart | cardiomyopathy | sarcomere | actin thin filament

Heart failure (HF) is a complex syndrome resulting from various upstream acquired or inherited diseases such as hypertension, ischemic heart disease, and genetically based cardiomyopathy, which are also influenced by environmental components and lifestyle choices (1, 2). Family-based rare variant analyses and genome-wide association studies (GWAS) have been instrumental approaches towards identifying disease causing or predisposing genetic variants (mutations) (3–5), although often the precise causative functions of the identified variants have been challenging to establish. However, modeling of newly identified variants in genetically modified mice is a proven method for suggesting causation (2, 6).

It is thought that about 1 in 500 individuals have an inherited cardiomyopathy that is roughly subdivided into two broad clinical phenotypes that includes hypertrophic cardiomyopathy (HCM) and dilated cardiomyopathy (DCM) (7). Familial HCM and DCM arise from greater than 1,500 distinct variants (mutations) in the genes that encode proteins of the sarcomere (8, 9). The sarcomere is the basic unit in muscle that generates contraction through a process known as excitation-contraction coupling in which the release of Ca^{2+} from internal stores and external sources directly binds the myofilament proteins to induce systole, while the sequestration of Ca^{2+} away from the myofilaments induces relaxation. In general, HCM-associated mutations sensitize the myofilaments towards Ca^{2+} adherence thereby generating greater initial force and prolonged mechanical relaxation. In contrast, DCM-associated mutations generally desensitize the myofilaments to a given amount of contractile Ca^{2+}, leading to reduced myofilament tension generation and faster relaxation (9, 10). Mutations in genes that impact the actin thin filament have also been associated with familial cardiomyopathies (11, 12).

Regulation of sarcomere length is primarily controlled at the level of the actin-containing thin filament (13). Tropomodulin-1 (TMOD1) is an important effector of this process where it caps the pointed end of the thin filaments (14–16). Leiomodin-2 (LMOD2) similarly resides at the pointed end of the actin thin filaments where it too regulates the length of the thin filament (16). For example, overexpression of TMOD1 in cardiac myocytes shortens thin filament length resulting in cardiomyopathy and HF (17, 18), while LMOD2 elongates the thin filament by competing with TMOD1 (19). Indeed, *Lmod2* gene-deleted mice have shorter thin filaments and show lethal cardiomyopathy (20).

Flightless-I homolog (*FLII*) is a member of gelsolin superfamily that is known to directly bind to filamentous actin (F-actin) and in some cases, sever the filament (21). The *flightless-I* gene in *Drosophila melanogaster*, which is the homologue of the single mammalian *FLII* gene, was originally shown to be required for indirect flight muscle function and proper sarcomere formation (22–25). More recently, it was reported that the formin Diaphanous collaborates with *flightless-I* to regulate thin filament length and sarcomere

Significance

Cardiovascular disease remains the leading cause of death in developed countries of the world. Human genetic analyses continue to identify novel genes that, when mutated, can underlie heart disease, although to infer causation genetically modified mouse models are now a requisite undertaking. Here we focused on the *Flightless-I homolog* (*FLII*) gene, associated with childhood-onset cardiomyopathy, and the low-frequency missense variant rs8821 in *FLII*, associated with cardiac remodeling. Using a series of genetically modified mice we show that the *Flii* gene regulates sarcomeric actin thin filament length by sequestering tropomodulin-1. Indeed, mice generated with the *FLII* human mutation (rs8821, R1243H) demonstrated shorter sarcomere thin filaments and susceptibility to cardiomyopathy. These results indicate that Flii is a critical regulator of cardiac sarcomere structure-function in vivo.

Author contributions: Y.K. and J.D.M. designed research; Y.K., A.J.Y., S.-C.L., M.A.S., and K.M.G. performed research; J.P.P. and J.D.M. analyzed data; and Y.K., J.P.P., and J.D.M. wrote the paper.

The authors declare no competing interest.

This article is a PNAS Direct Submission.

[1]To whom correspondence may be addressed. Email: jeff.molkentin@cchmc.org.

This article contains supporting information online at https://www.pnas.org/lookup/suppl/doi:10.1073/pnas.2213696120/-/DCSupplemental.

Published May 1, 2023.

size in *Drosophila* (26). Here, we focused on the *Flii* gene with unknown function in the mammalian heart and a human *FLII* variant, rs8821 (27). In addition to the familial evidence showing association between *FLII* variants and childhood-onset cardiomyopathy, we analyzed multiple previously published human GWAS data sets that contained the rs8821 polymorphism (28–33), which is a coding missense variant within the *FLII* gene (R1243H). Since very little is understood of Flii function in the heart, the mouse was used in both gain- and loss-of-function genetic studies, as well as by directly modeling the syntenic missense change from the human variant to the mouse *Flii* gene (R1245H). We show that Flii functions at the level of the cardiac sarcomere where it is associated with the actin-containing thin filament to regulate its length. Our results suggest that the human *FLII* variant likely predisposes to cardiomyopathy through alterations in sarcomere structure-function.

Results

***FLII* Gene and rs8821 Variant.** *FLII* has been identified in family studies as a potential cause of cardiac dysfunction, with homozygous carriers of variants in the gelsolin-like domain (GLD) at the C-terminus of the protein developing childhood-onset cardiomyopathy (5). In addition to prior evidence from familial studies, we sought population-level human genetic evidence to further understand *FLII*'s relationship with cardiac phenotypes. Using the gnomAD database (27), we focused on variants in *FLII* whose minor allele frequencies (MAF) were between 1 to 5% with predicted functionally damaging effects by bioinformatic algorithms including Polyphen and SIFT analyses. Only rs8821, which encodes an R1243H amino acid substitution, fit those criteria. To explore the association of rs8821 variant in cardiac phenotypes and diseases, we queried the cardiovascular disease knowledge portal (https://cvd.hugeamp.org/) and identified nominal associations between the *FLII* rs8821 variant and multiple cardiovascular diseases and phenotypes in humans (*SI Appendix,* Table S1). For example, the CHARGE QRS interval exome chip GWAS and the TOPMed 2021 Electrocardiogram GWAS showed that rs8821 was nominally associated with a narrower QRS interval (effect estimate = −0.40, P = 6.0E-3; and effect estimate = −1.38, P = 1.0E-03, respectively) (28, 29). The *FLII* rs8821 variant was also nominally associated with an enlarged left ventricle and reduced ejection fraction (EF) measured by cardiac magnetic resonance in a GWAS of 36,042 UK Biobank participants (30, 31) as shown in *SI Appendix,* Fig. S1*A* indicating that this variant was associated with cardiac remodeling. A multi-ethnic atrial fibrillation (AFib) GWAS in 2018 reported that rs8821 was associated with an increased risk of AFib (odds ratio [OR] 1.09, P = 1.4E-03) in more than half a million individuals (32). Two HF GWAS—FinnGen 2018 GWAS with 3,116 participants (https://www.finngen.fi/en) and HERMES HF GWAS with 909,806 participants (33) showed directionally concordant effects for rs8821 as well. The OR for HF was 1.47 (P = 7.4E-03) in FinnGen and 1.05 (P = 0.049) in HERMES. These data suggest that this variant increases the risk of AFib and HF. The gnomAD database (27) showed a MAF of rs8821 as 0.0175 in the total human population, while European descent populations showed a MAF of 0.0267 indicating that 7 in 10,000 people could be rs8821 homozygotes. The *FLII* R1243H missense change due to rs8821 resides within the GLD at the C-terminus of this protein, which is critical for actin interaction (34–36). As noted above, two other human homozygous variants in the GLD of *FLII* have been suggested to underlie childhood DCM (5), also supporting the importance of the Flii protein in cardiac structure-function relationships (*SI Appendix,* Fig. S1*B*).

Analysis of *Flii* Cardiac-Specific Gene-Deleted Mice. Given the human genetic evidence, we investigated the potential for a causal relationship between *FLII* and cardiac phenotypic alternations using genetic modeling in the mouse. However, very little is known of Flii expression or function in the heart, other than the observation in *Drosophila* with mutations in this gene homologue (*flightless-I*) that cause lethal dysgenesis of the indirect flight muscles with disrupted sarcomeric structure (25). However, because germline *Flii* gene-deleted mice are embryonic lethal (37), here we generated mice with loxP sites targeting exons 8 to 14 of the *Flii* gene, which with Cre-mediated deletion permits a loss-of-function analysis in any desired tissue (Fig. 1*A*). Using an early embryonic deletion approach specific to the heart with the *Nkx2.5-Cre* knock-in allele, we failed to observe viable $Flii^{fl/fl}$ homozygotes at 6 d after birth, suggesting developmental lethality (Fig. 1*B*). However, using the cardiac-specific and postnatal expressed α-myosin heavy chain (αMHC) promoter to drive Cre expression by transgenesis (38), we now obtained viable mice (Fig. 1*C*). Western blot analysis from the hearts of these mice at 16 wk of age showed effective deletion of the protein (Fig. 1*D*). By 16 wk of age $Flii^{fl/fl\text{-}\alpha MHC\text{-}Cre}$ mice showed cardiac hypertrophy (Fig. 1*E*) with a reduction in cardiac ventricular performance measured by echocardiography (Fig. 1*F*). Exact measurement of ventricle weight to body weight ratios showed a significant increase at 16 wk of age in $Flii^{fl/fl\text{-}\alpha MHC\text{-}Cre}$ mice versus $Flii^{+/+\text{-}\alpha MHC\text{-}Cre}$ or $Flii^{fl/fl}$ control lines (Fig. 1*G*). This enlargement was associated with HF as *Flii* heart-specific deleted mice showed increases in lung weight (Fig. 1*H*), indicating congestion, as well as premature lethality in early adulthood (Fig. 1*I*). To investigate the potential cellular and structural defects in the heart associated with *Flii* cardiac-specific deletion we performed electron microscopy of the heart at 7 wk of age, as well as in a few rare mice that lived to 6 mo of age. The analysis showed ultrastructural alterations in the 7-wk heart with ectopic regions of aggregated and repetitive Z-line structures (*SI Appendix,* Fig. S2, black arrows in *Top Right* panel), while by 6 mo of age there was profound sarcomeric dysgenesis throughout the heart (*SI Appendix,* Fig. S2, white arrows), as well as alterations in the structure of the nucleus (asterisk) and intercalated discs (*SI Appendix,* Fig. S2, black arrows in *Bottom Right* panel).

We also investigated $Flii^{+/-}$ (heterozygous) gene-targeted mice that have a full null allele for *Flii* (*Materials and Methods*), which showed no reduction in total levels of Flii (*SI Appendix,* Fig. S3*A*). These results are important as they indicate that heterozygosity in *Flii*, is not pathologic to the heart, and because Flii appears to be primarily a sarcomeric protein, half the mRNA level does not reduce total protein levels, as previously observed with other sarcomeric proteins in the heterozygous deleted state (39, 40). We also failed to observe abnormalities in cardiac structure-function of the adult heart of $Flii^{+/-}$ mice with aging to 16 wk, or in 16-wk-old mice subjected to 8 wk of prior pressure overload stimulation with transverse aortic constriction (TAC) (*SI Appendix,* Fig. S3 *B–F*). However, deletion of both alleles of *Flii* from the hearts of $Flii^{fl/fl}$ adult mice beginning at 4 wk of age using the tamoxifen-inducible αMHC-MerCreMer transgene, which reduced Flii protein by 70%, did cause a pathologic effect such that by 11 wk of age *Flii*-deleted mice had cardiac hypertrophy, and with 3 wk of TAC stimulation there was significantly greater hypertrophy that transitioned into HF indicated by lung congestion (*SI Appendix,* Fig. S4). These later results are important because they indicate that Flii is required for homeostasis in the adult mouse heart, and that the early adult lethal phenotype observed in constitutive $Flii^{fl/fl\text{-}\alpha MHC\text{-}Cre}$ mice (Fig. 1*I*) is not exclusively due to a postnatal developmental effect within the heart.

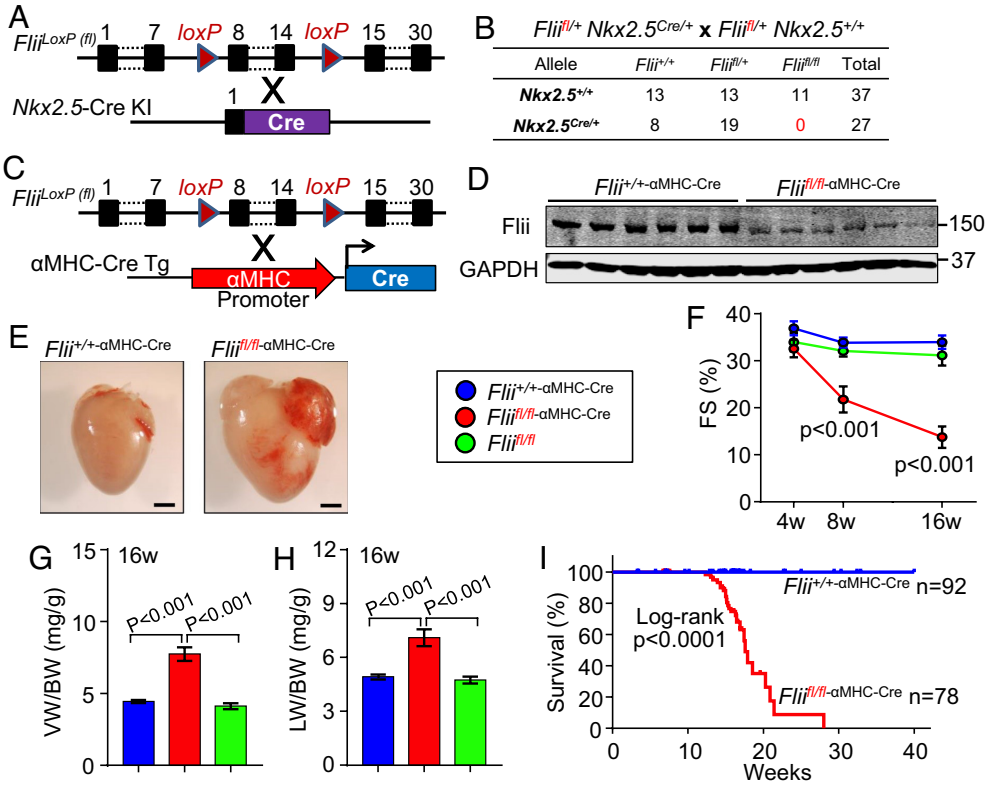

Fig. 1. Cardiomyocyte-specific *Flii* gene deletion in mice results in cardiomyopathy and premature death. (*A*) Genetic loci diagram of the strategy to generate cardiomyocyte-specific *Flii* gene deletion in mice with the *Nkx2.5*-Cre knock-in (KI) line. (*B*) Numbers of observed progeny 6 d after birth from $Flii^{fl/+}$ $Nkx2.5^{Cre/+}$ mice crossed with $Flii^{fl/+}$ $Nkx2.5^{+/+}$ mice. (*C*) Genetic loci diagram of the strategy to generate cardiomyocyte-specific *Flii* gene deletion in mice with the αMHC-Cre transgenic line ($Flii^{fl/fl\text{-}\alpha MHC\text{-}Cre}$) mice. (*D*) Western blot of Flii from hearts of $Flii^{+/+\alpha MHC\text{-}Cre}$ (control) and $Flii^{fl/fl\text{-}\alpha MHC\text{-}Cre}$ mice at 16 wk of age. Glyceraldehyde 3-phosphate dehydrogenase (GAPDH) is a processing and loading control. Numbers indicate molecular weights (kDa) (*E*) Photographic images of hearts from control (*Left*) and $Flii^{fl/fl\text{-}\alpha MHC\text{-}Cre}$ mice (*Right*) at 16 wk of age. Black bars indicate 2 mm. (*F*) Echocardiographic assessment of fractional shortening (FS) in the indicated groups of mice at the indicated ages. $Flii^{+/+\text{-}\alpha MHC\text{-}Cre}$ (blue) n = 9; $Flii^{fl/fl\text{-}\alpha MHC\text{-}Cre}$ (red) n = 10; $Flii^{fl/fl}$ (green) n = 8. *P* value: $Flii^{fl/fl\text{-}\alpha MHC\text{-}Cre}$ vs. $Flii^{+/+\text{-}\alpha MHC\text{-}Cre}$ or $Flii^{fl/fl}$ at same time points. Data is shown as mean ± SEM. (*G* and *H*) Ventricular Weight/Body Weight (VW/BW) ratio (*G*) and Lung Weight/Body Weight (LW/BW) ratio (*H*) at 16 wk of age in the indicated groups of mice. $Flii^{+/+\text{-}\alpha MHC\text{-}Cre}$ (blue) n = 19; $Flii^{fl/fl\text{-}\alpha MHC\text{-}Cre}$ (red) n = 20; $Flii^{fl/fl}$ (green) n = 8. Data are shown as mean ± SEM. (*I*) Survival curves of $Flii^{fl/fl\text{-}\alpha MHC\text{-}Cre}$ mice (red, n = 78) and $Flii^{+/+\text{-}\alpha MHC\text{-}Cre}$ mice (blue, n = 92).

Analysis of the Flii Interactome Suggests it Is a Sarcomeric Regulatory Protein. We next sought to examine the function of Flii within cardiomyocytes by investigating its interactome with other proteins. We began with an unbiased analysis using 293T cells as a platform given the ease of expressing protein domains in this system (Fig. 2*A*). For this analysis we generated full-length mouse Flii with a Flag-tag. Overexpression of Flii followed by Flag-dependent purification and mass spectrometry proteomics identified actin, as previously reported (35, 36), but also tropomodulin-3 (Fig. 2*B*). Tropomodulin (TMOD) was selected for further investigation given its known role in actin filament assembly and length determination (17, 41), and because previous studies have linked Flii function to regulation of actin networks in various cell types (34, 36, 42, 43). Using the N-terminal leucine-rich repeats (LRR), or the C-terminal GLD of Flii with Flag-tags (23) (Fig. 2*C*), molecular dissection of this interaction in 293T cells showed that the ubiquitously expressed TMOD3 protein was associated specifically with the GLD region of Flii, but not the LRR domain (Fig. 2*D*). We extended this analysis to cultures of primary neonatal rat ventricular cardiomyocytes (NRVMs), which identified muscle-enriched TMOD1 as interacting with Flii, and more specifically, the GLD region (Fig. 2*E*). Given these results we investigated heart protein extracts from $Flii^{fl/fl\text{-}\alpha MHC\text{-}Cre}$ mice to determine if proteins associated with the actin thin filament might be altered, and indeed, we identified a significant increase in expression of leiomodin-2 (LMOD2) (Fig. 2 *F* and *G*) at 16 wk old of age, which functions to extend sarcomeric actin thin filament lengths in vivo (20, 44). This was also of interest because confocal microscopic analysis of sarcomeres in the hearts of $Flii^{fl/fl\text{-}\alpha MHC\text{-}Cre}$ mice showed a reduction in sarcomeric distance between the Z-lines, which was due to a direct shortening of the entire thin filament structure across the Z-line (Fig. 2 *H–J* and *SI Appendix*, Fig. S5*A*). Given that *Lmod2* null mice show shorter thin filaments and lethal cardiomyopathy in the juvenile period (20), it is reasonable to suggest that LMOD2 upregulation in the $Flii^{fl/fl\text{-}\alpha MHC\text{-}Cre}$ mice is a compensatory effect aimed at elongating thin filaments in the $Flii^{fl/fl\text{-}\alpha MHC\text{-}Cre}$ heart.

AAV9-LMOD2 Rescues the Phenotype of Flii Heart-Deleted Mice. Flii has been shown to directly regulate filamentous actin assembly in vitro and in vivo (26, 34, 36). Indeed, we also determined that recombinant Flii, when added to G-actin in solution with the barbed-end capping proteins CapZα1 and CapZβ, enhanced filamentous actin assembly in a concentration dependent manner (Fig. 3 *A* and *B*). Moreover, because Flii is associated with TMOD1 in the heart, and because TMOD1 binds the pointed end of filamentous actin and results in sarcomeric thin filament shortening in the heart (16, 41), we hypothesized that a primary function of Flii was to participate in thin filament length dynamics. To this end, we generated a recombinant cardiac troponin T (cTnT) promoter driven adeno-associated virus-9 (AAV9) vector to overexpress LMOD2 in cardiomyocytes of the hearts of $Flii^{fl/fl\text{-}\alpha MHC\text{-}Cre}$ mice, in an attempt to rescue the lethality associated with thin filament length shortening, in part, because LMOD2

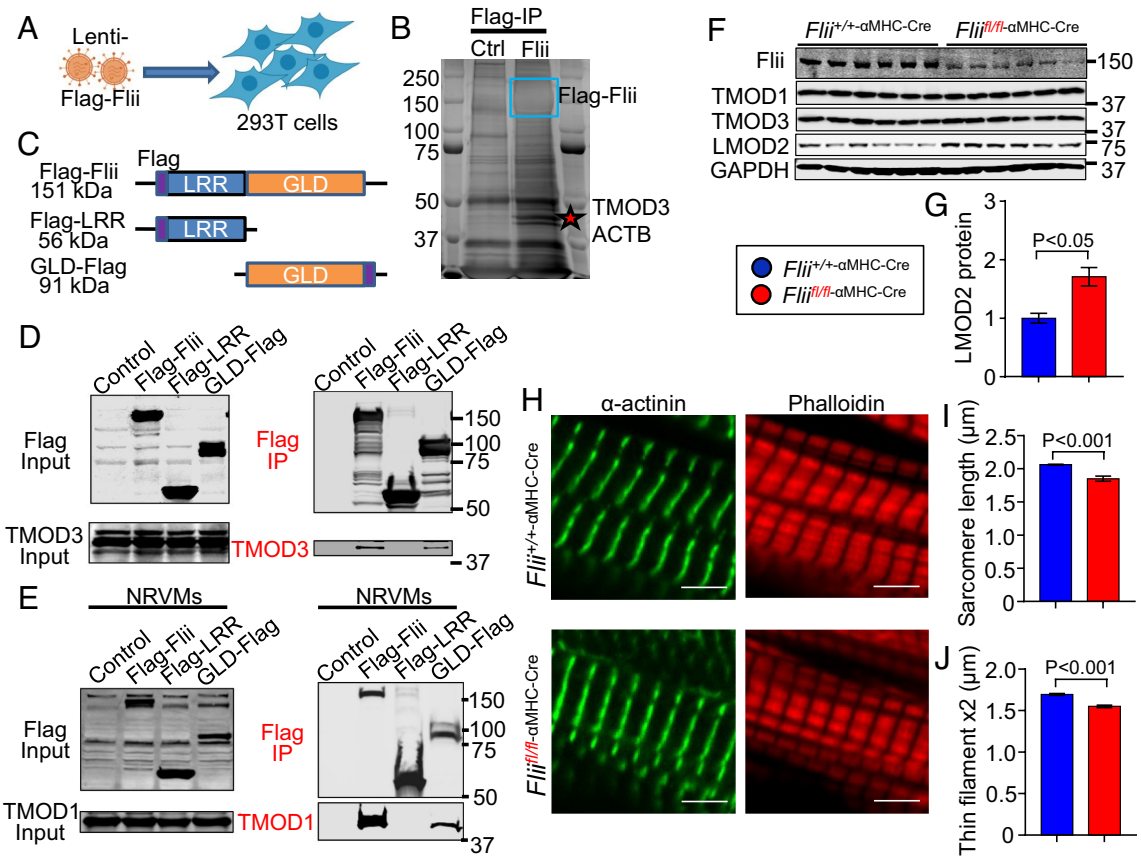

Fig. 2. Flii is a sarcomeric protein that regulates the actin thin filament. (*A*) Strategy to overexpress Flag-Flii protein in 293T cells with lentivirus. (*B*) Flag-based immunoprecipitation (IP) from infected 293T cells subjected to PAGE and silver staining, which shows Flag-Flii protein (blue box) and the proteins pulled down with it (red star shows the position of TMOD3 and ACTB proteins identified by mass spectrometry). (*C*) Diagram of the constructs used in IP-Westerns shown in *D* and *E*. Flii contains a leucine-rich repeat (LRR) domain and gelsolin-like domain (GLD). (*D* and *E*) IP-Westerns from *D* 293T or (*E*) neonatal rat ventricular myocyte (NRVM) cell lysates infected with lentivirus expressing the indicated Flag-tagged Flii protein or domains. The *Left* panels are western blots for the indicated protein from protein inputs, while the *Right* panels are westerns after Flag IP for Flag or TMOD1 or TMOD3 as shown. (*F*) Westerns of Flii, TMOD1, TMOD3, LMOD2, and GAPDH (loading control) from heart lysates generated from the indicated genotype of mice at 16 wk of age. Numbers indicate molecular weights (kDa) in *B* and *D*–*F*. The Flii and GAPDH blots were also shown in Fig. 1*D*. (*G*) Quantification of the LMOD2 Westerns as shown in panel *F*. Blue is *Flii*$^{+/+\text{-}\alpha MHC\text{-}Cre}$ (control) mice n = 11; Red is *Flii*$^{fl/fl\text{-}\alpha MHC\text{-}Cre}$ mice n = 9. (*H*) Representative immunohistochemical images of α-actinin (green) and Phalloidin (red) from hearts of the indicated groups of mice at 16 wk of age. (Scale bars indicate 4 μm.) (*I* and *J*) Quantification of sarcomere length (*I*) and thin filament length (*J*) from immunohistochemical images as shown in *H*. Control n = 5 and experimental n = 6. Data are mean ± SEM.

overexpression is known to lengthen sarcomeric thin filaments in the heart (Fig. 3*C*) (20, 44). After injection in neonates with AAV9-LMOD2 at P6, western blotting confirmed LMOD2 upregulation at 4 wk of age (Fig. 3 *D* and *E*) in the heart. The upregulation was sufficient to partially rescue the reduction in cardiac ejection fraction, the increase in cardiac hypertrophy at 16 wk of age, and the degree of premature lethality due to cardiac-specific *Flii* deletion (Fig. 3 *F*–*H*). Mechanistically, LMOD2 overexpression increased sarcomere thin filament length at baseline in control hearts, but more importantly, it reversed the shortening of thin filaments in hearts of *Flii*$^{fl/fl\text{-}\alpha MHC\text{-}Cre}$ mice (Fig. 3*I*). These results indicate that a substantial component of the pathology associated with *Flii* deletion from the mouse heart is due to a pathologic reduction in sarcomere thin filament length.

Generation of Cardiac-Specific Flii WT and Mutant Transgenic Mice. To begin to examine how the human rs8821 variant resulting in R1243H amino acid substitution might be pathologic, we generated parallel cardiac-specific transgenic mice to overexpress WT mouse Flii or the homologue to the rs8821 polymorphism that codes for R1245H (mutant) in the mouse, which is syntenic between the two species (Fig. 4*A*). Western blotting from a low and high transgenic line for each strategy showed matched overexpression (Fig. 4*B*). Overexpression of WT Flii had no impact on cardiac function or baseline hypertrophy at 16 wk of age, although overexpression of the R1245H mutant resulted in a mild reduction in ejection fraction (EF) measured by echocardiography in the heart at this same age (Fig. 4*C*), but without a change in ventricle weight normalized to body weight (Fig. 4*D*). However, overexpression of the Flii-mutant caused a significant shortening of sarcomeric thin filament length, but not with Flii WT (*SI Appendix,* Fig. S5 *B* and *C*). Similarly, 8 wk of pressure overload had no deleterious effect in Flii WT transgenic mice at 16 wk of age as assessed by measurements of EF, ventricle weight to body weight ratio and lung weight to body weight ratio, while the Flii mutant transgenic mice showed HF as suggested by lung congestion (*SI Appendix,* Fig. S6). These results suggest that this R1245H alteration in Flii can have a dominant effect in altering sarcomeric structure, which predisposes to cardiomyopathy.

More interestingly, we identified a profound alteration in Flii immunolocalization in the hearts of mutant transgenic mice compared to WT overexpressors (Fig. 4 *E*–*G*). Because the existing Flii antibodies are unable to detect endogenous Flii in cardiac immunohistochemistry, we used Flag antibody to detect the tagged version of WT and mutant Flii expressed in the transgenic

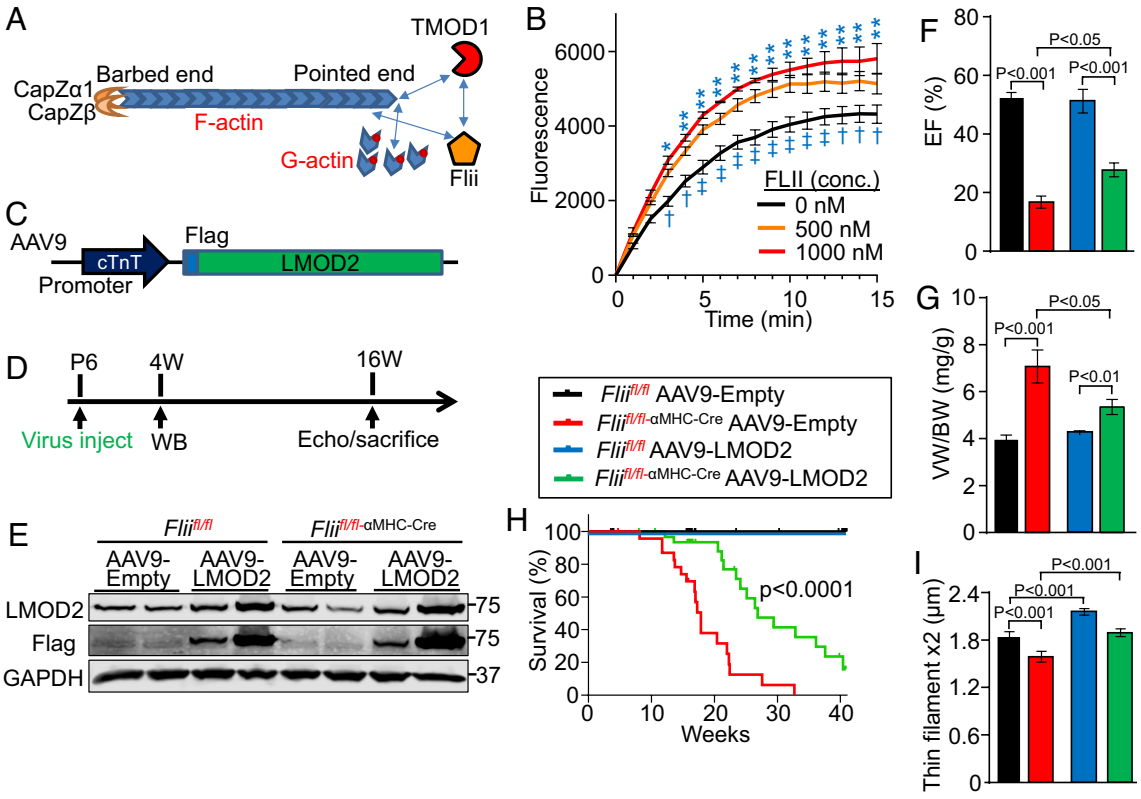

Fig. 3. Flii regulates actin polymerization and sarcomeric actin thin filament length in affecting cardiomyopathy predisposition. (*A*) Schematic of an in vitro G-actin polymerization assay to generate F-actin at the pointed end given capping of the barbed end with CapZα1 and CapZβ. Flii and TMOD1 proteins were also added. The polymerization is monitored by pyrene fluorescence. (*B*) Actin polymerization assay with different concentrations of Flii in the presence of TMOD1. $^{\ddagger}P < 0.05$ 0 nM vs. 500 nM Flii; $^{\ddagger}P < 0.01$ 0 nM vs. 500 nM Flii; $^{*}P < 0.01$ 0 nM vs. 1000 nM Flii; $^{**}P < 0.001$ 0 nM vs. 1000 nM Flii. Data are shown as mean ± SEM. (*C*) Diagram of cardiac troponin T promoter (cTnT)-AAV9 construct harboring Flag-tagged LMOD2. (*D*) Timeline of the rescue experiment in $Flii^{fl/fl\text{-}\alpha MHC\text{-}Cre}$ mice infected with AAV9-LMOD2 or an empty control AAV9 virus. (*E*) Western blots from hearts of mice at 4 wk of age for LMOD2, Flag and GAPDH (loading control) from the indicated groups of mice. Numbers indicate molecular weights (kDa) (*F*) Echocardiography measured ejection fraction (EF) at 16 wk of age in the groups of mice shown in the legend above panel *H*. $Flii^{fl/fl}$ +AAV9-Empty vector (black) n = 5; $Flii^{fl/fl\text{-}\alpha MHC\text{-}Cre}$ + AAV9-Empty vector (red) n = 11; $Flii^{fl/fl}$ + AAV9-LMOD2 (blue) n = 8; $Flii^{fl/fl\text{-}\alpha MHC\text{-}Cre}$ + AAV9-LMOD2 (green) n = 13. (*G*) Ventricular Weight/Body Weight (VW/BW) ratio in the indicated groups of mice at 16 wk of age. Black n = 5; red n = 5; blue n= 15; green n = 7. (*H*) Survival curves of the indicated four treatment groups of mice. Black n = 14; red n = 24; blue n = 35; green n = 32. $P < 0.0001$ with log-rank test: red vs. green. (*I*) Quantification of total thin filament length across the Z-line in the indicated groups of mice at 16 wk of age. Black n = 7; red n = 7; blue n = 4; green n = 3. Graphs are shown as mean ± SEM.

mice. For co-staining, we used TMOD1 to show the free ends of the thin filaments in the heart, which resides at the M-band, where WT Flii is highly concentrated. WT Flii also binds throughout the entire length of the thin filament in a manner that partially excludes the Z-line (*Top* panels in Fig. 4 *E*–*G* and *SI Appendix*, Fig. S7 *A*, *B*, *D* and *F*). In sharp contrast, the Flii mutant protein has an opposing localization pattern within the sarcomere, where it is mostly restricted to the Z-line and coincident with α-actinin, unable to interact with TMOD1 or localize to the M-band (*Bottom* panels in Fig. 4 *E* and *F* and *SI Appendix*, Fig. S7 *A*, *C*, *E* and *G*). Indeed, the Flii mutant protein localizes at the center of the immunohistochemical staining pattern of phalloidin (*Bottom* panels in Fig. 4*G* and *SI Appendix*, Fig. S7 *A* and *G*). By comparison, WT Flii colocalizes with phalloidin throughout much of the length of the thin filament (*Top* panels in Fig. 4*G* and *SI Appendix*, Fig. S7*F*). To exclude a possibility of a non-specific signal due to the antibodies used, histological sections from Flii mutant transgenic hearts were stained with secondary antibody only, while histological sections from non-transgenic hearts were stained with primary and secondary antibodies, which collectively ruled out non-specific staining (*SI Appendix*, Fig. S7*A*). Thus, the change in amino acid R1245H within Flii disrupts its normal sarcomeric localization and causes an ectopic pattern of enrichment to the Z-line. This Flii mutant protein also failed to interact with TMOD1 protein from protein lysates generated from neonatal rat heart ventricular myocytes in which Flii mutant protein was overexpressed, while WT Flii showed a strong interaction (Fig. 4*H*). These results suggest that the homologue of the human rs8821 variant in mice alters the in vivo localization and interacting characteristics of Flii in the heart.

Generation of Mouse Flii Knock-in Model for the rs8821 Variant. While analysis of mice with deletion of *Flii* in the heart, as well as transgene-mediated overexpression provided important mechanistic information as to the function of this protein in regulating thin filament dynamics, we also generated gene-targeted mice with the same conserved amino acid substitution identified in the human rs8821 variant. We used CRISPR/Cas9 technology to generate a germline single amino acid substitution at amino acid 1,245 (R to H) in mouse *Flii*, and while these mice were normal as young heterozygotes, the homozygotes showed reduced cardiac function by 16 wk of age (Fig. 5 *A* and *B*). Considering the human phenotypes associated with the rs8821 variant that manifest later in life, we also assessed cardiac systolic function in mice at 52 wk of age and observed that both heterozygous and homozygous displayed reduced cardiac function (Fig. 5*C*). Furthermore, 8-wk-old $Flii^{R1245H/R1245H}$ mice subjected to 8 wk of TAC showed significantly worse cardiac function with greater cardiac hypertrophy, greater lung congestion, and premature lethality compared with WT and $Flii^{R1245H/+}$ heterozygous controls (Fig. 5 *D*–*G*). Importantly, sham

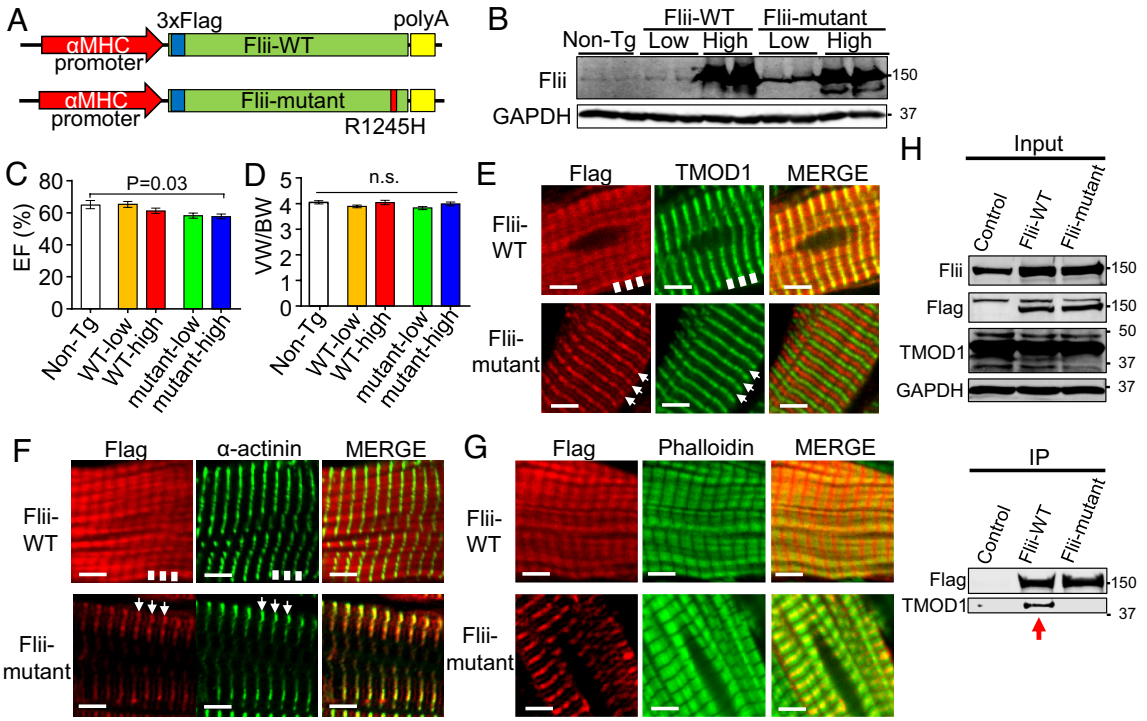

Fig. 4. Generation and characterization of WT and mutant Flii transgenic mice. (*A*) Diagram of the transgenes used to generate Flag-tagged Flii-WT and -mutant heart-specific mice. The rs8821 polymorphism in humans (R1243H) corresponds to R1245H in the mouse Flii protein. (*B*) Westerns of Flii and GAPDH from hearts of non-transgenic (Non-Tg) and the four different Flii-based transgenic lines. (*C* and *D*) Echocardiography measured ejection fraction (EF) and Ventricular Weight to Body Weight (VW/BW) ratios at 16 wk of age in the indicated transgenic lines of mice. EF data: Non-Tg n = 9; WT-low n = 10; WT-high n = 13; mutant-low n = 6; mutant-high n = 15. VW/BW data: Non-Tg n = 33; WT-low n = 19; WT-high n = 14; mutant-low n = 11; mutant-high n = 16. n.s. indicates not significant. Graphs are shown as mean ± SEM. (*E–G*) Representative immunohistochemical images of Flag (red) and TMOD1, α-actinin, or Phalloidin (green) in hearts of Flii-WT versus Flii-mutant transgenic mice at 16 wk of age. The solid white boxes show the position of greatest concentration of Flii-WT (Flag) reactivity across the panels, while the white arrows show the position of enriched Flii-mutant (Flag) protein. (Scale bars are 4 μm.) (*H*) Westerns after Flag-immunoprecipitation (IP) from lysates of neonatal rat ventricular myocytes (NRVMs) infected with recombinant lentivirus to overexpress β-galactosidase (control), Flag-Flii-WT, or Flag-Flii-mutant. *Top* panels are westerns of input for Flii, Flag, TMOD1 and GAPDH, while the *Bottom* panels are IP-Western blots of Flag and TMOD1. Numbers indicate molecular weights (kDa).

mice at 16 wk of age showed reduced thin filament length in the hearts of *Flii*$^{R1245H/R1245H}$ homozygous mice compared with the two control groups (Fig. 5*H*).

The reduction in sarcomeric thin filament length in hearts of *Flii*$^{R1245H/R1245H}$ homozygous mice is predicted to reduce contraction dynamics due to non-optimized overlap between the thin and thick filaments, as mechanistically shown previously by manipulating TMOD1 and LMOD2 expression in cardiomyocytes (19, 20, 44). This disruption of optimized thick and thin filament overlap mimics aspects of how other known variants in sarcomeric genes leads to either HCM or DCM due to changes in Ca^{2+} sensitivity of contractile activity (10). To further reduce the Ca^{2+} sensitivity in the *Flii*$^{R1245H/R1245H}$ homozygous mice and to explore these mechanistic underpinnings, we crossed the *Flii*$^{R1245H/R1245H}$ mice into a mouse model of DCM due to reduced Ca^{2+} sensitivity of an overexpressed cardiac troponin C mutant (10). The characteristic adulthood lethality in cTnC-I61Q transgenic mice showed an even earlier lethality with the addition of the *Flii*$^{R1245H/R1245H}$ homozygous alleles, compared with control crosses (Fig. 5*I*). These results suggest that the *Flii* homozygous mutation and shortening of the thin filament further compromises contractile activity associated with the cTnC-I61Q transgene through the same presumed mechanism revolving around reduced contractile activity that occurs with DCM.

To further investigate the mechanistic effects of the R1245H mutation in mouse *Flii*, we examined actin polymerization dynamics in vitro between WT Flii and the R1245H mutant protein (Fig. 5*J*). The data show that WT Flii again augmented G-actin polymerization into F-actin in a concentration dependent manner, while Flii-R1245H mutant protein antagonized polymerization (Fig. 5*K*). This result is also interesting given the other interactions between Flii and known binding proteins that we observed to also be disrupted by the R1245H mutation (*SI Appendix,* Fig. S8). More specifically, we used whole heart protein extracts from αMHC-Flii-WT or Flii-mutant transgenic mice for Flag-based immunoprecipitation and mass spectrometry proteomics, which identified vinculin, gelsolin, LMOD2, and desmin (*SI Appendix,* Fig. S8*A*). Confirmation immunoprecipitation followed by western blotting verified these interactions from the hearts of Flii-WT transgenic mice, yet these same proteins either did not interact or only weakly interacted with Flii-R1245H mutant protein (*SI Appendix,* Fig. S8*B*). This provides further evidence that Flii functions within the heart to regulate sarcomeric structure at the level of the thin filament, in part by direct interactions with other thin filament proteins as well as select cytoskeletal proteins that themselves link to the sarcomeres. Thus, the identified variant in human *FLII*, which we modeled in the mouse (R1245H), disrupts Flii localization and its interactome, which predisposes to cardiomyopathy due to alterations in thin filament length regulation.

Discussion

Previous work has shown that Flii regulates cortical/cytoskeletal actin network dynamics, such as with cell movement and healing in a wide array of cell types (34, 36, 37, 42, 43, 45). However, we provide evidence that Flii also directly regulates the more highly organized structure of the sarcomeric α-actin network within the

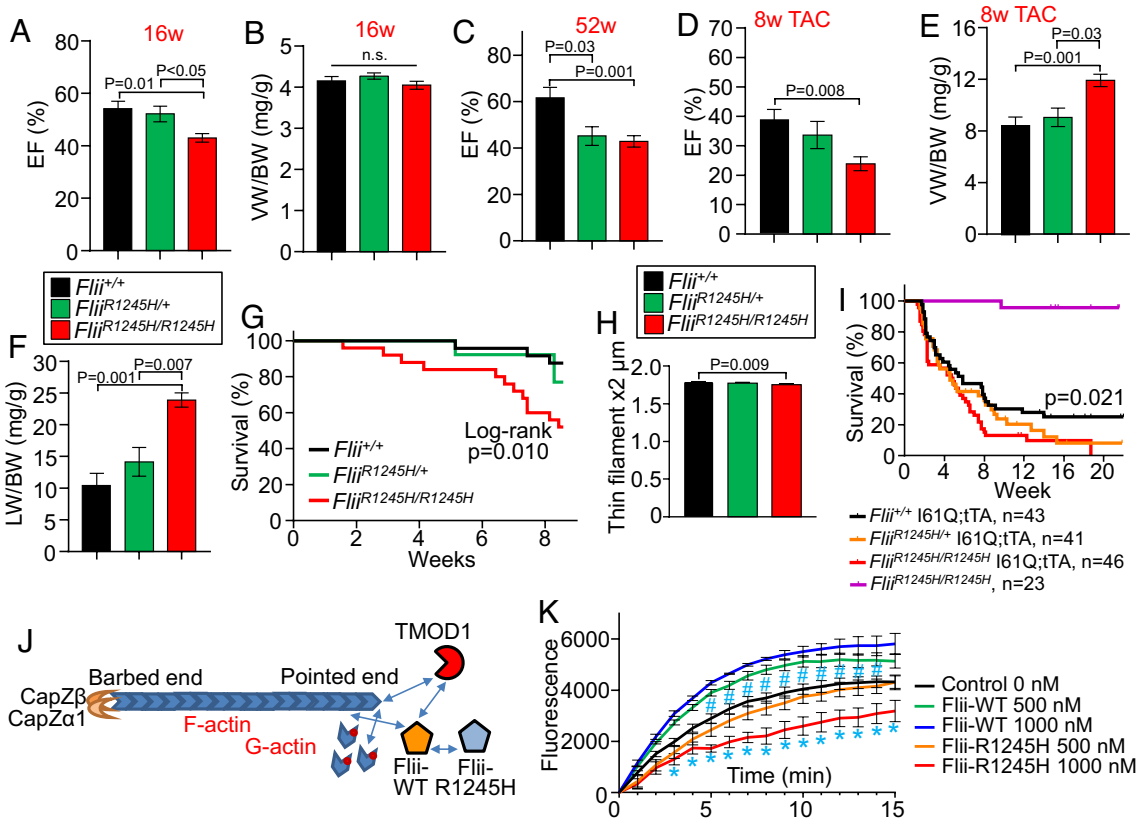

Fig. 5. *Flii*-R1245H knock-in mice model human DCM like alterations due to rs8821. (*A*) Echocardiography measured ejection fraction (EF) in the three indicated genotypes of mice at baseline at 16 wk of age. $Flii^{+/+}$ n = 18; $Flii^{R1245H/+}$ n = 18; $Flii^{R1245H/R1245H}$ n = 17. (*B*) Ventricular Weight/Body Weight (VW/BW) ratio at baseline (16 wk of age). $Flii^{+/+}$ n = 15; $Flii^{R1245H/+}$ n = 20; $Flii^{R1245H/R1245H}$ n = 16. n.s. indicates not significant. (*C*) Echocardiography measured EF at baseline at 52 wk of age. $Flii^{+/+}$ n = 10; $Flii^{R1245H/+}$ n = 5; $Flii^{R1245H/R1245H}$ n = 14. (*D–F*) EF (*D*), VW/BW ratio (*E*), and Lung Weight/Body Weight (LW/BW) ratio (*F*) at 8 wk after transverse aortic constriction (TAC). 16 wk of age total. $Flii^{+/+}$ n = 16; $Flii^{R1245H/+}$ n = 10; $Flii^{R1245H/R1245H}$ n = 13. (*G*) Survival curves after TAC surgeries. $Flii^{+/+}$ (black) n = 30; $Flii^{R1245H/+}$ (green) n = 16; $Flii^{R1245H/R1245H}$ (red) n = 33. *P* = 0.0102 with log-rank test: $Flii^{+/+}$ vs. $Flii^{R1245H/R1245H}$. (*H*) Quantification of total thin filament length across the Z-line. $Flii^{+/+}$ n = 3; $Flii^{R1245H/+}$ n = 4; $Flii^{R1245H/R1245H}$ n = 4. All data are mean ± SEM for *A–F* and *H*. (*I*) Survival curves of $Flii^{R1245H/R1245H}$ knock-in mice crossed with cTnC-I61Q;tTA double transgenic mice. $Flii^{R1245H/R1245H}$ n = 23, $Flii^{+/+}$;cTnC-I61Q;tTA n = 43, $Flii^{R1245H/+}$;cTnC-I61Q;tTA n = 41, $Flii^{R1245H/R1245H}$;cTnC-I61Q;tTA n = 46. *P* = 0.0211 with log-rank test: $Flii^{+/+}$;cTnC-I61Q;tTA vs. $Flii^{R1245H/R1245H}$;cTnC-I61Q;tTA. (*J*) Schematic of an in vitro G-actin polymerization assay to generate F-actin at the pointed end given capping of the barbed end with CapZα1 and CapZβ. Flii-WT or Flii-R1245H and TMOD1 proteins were added. The polymerization is monitored by measuring the pyrene fluorescence. (*K*) Results of the actin polymerization assay with the indicated concentration of Flii-WT or Flii-R1245H protein. $^{\#}P < 0.05$ 500 nM Flii-WT vs. 500 nM Flii-R1245H. $^{*}P < 0.001$ 1000 nM Flii-WT vs. 1000 nM Flii-R1245H. Data are shown as mean ± SEM.

heart, which generates the thin filaments that couple with the myosin containing thick filaments to generate contractile activity. Here we showed that Flii regulates sarcomeric actin dynamics in cardiomyocytes, which is typically composed almost exclusively of cardiac or skeletal α-actin. A paucity of literature exists that examined the function of Flii in the heart (or muscle) even though the originating mutation discovery in *Drosophila* in the *flightless-I* gene showed sarcomere disorganization within the indirect flight muscles as the cause of lethality (22–26). Indeed, the identified human variant in *FLII* that predisposes to cardiomyopathy is further evidence supporting a critical role for this protein in regulating the structure-function of the sarcomere. Future studies will be required to dissect the exact biochemical mechanism whereby Flii works with or competes with LMOD2 and TMOD1 at the pointed end of the actin thin filament, and how other known Flii interacting sarcomeric proteins might be involved in this process.

There are hundreds of genetic variants across dozens of genes encoding sarcomeric proteins that are linked to genetically-influenced cardiac disease states, most of which can be classified as HCM or DCM (9, 10). In general, those sarcomere gene encoding variants (mutations) that reduce contractile rigor for a given amount of Ca^{2+} appear to cause or predispose to a DCM phenotype, while variants that increase contractile rigor for a given amount of Ca^{2+} are associated with HCM. Here we identified a change in the length of the sarcomeric actin containing thin filament in both *Flii* gene-deleted mice and the rs8821 modeling knock-in variant, which is predicted to alter the biophysical properties of the sarcomeres. Indeed, deletion of LMOD2 in mice leads to shortening of the actin thin filaments in the heart and cardiomyopathy (20), which is consistent with the cardiomyopathy observed here in *Flii* heart-specific null mice. This effect of *Flii* R1245H variant is predicted to reduce force generation within cardiomyocytes at the level of cross-bridge cycling, as shown previously in LMOD2 and TMOD1 altered mice or myocytes in culture (16, 17, 19, 44).

One of the more remarkable findings of the current study is that a single amino acid substitution of R1245H in the far C-terminus of mouse *Flii*, which resides within the GLD region, changes the localization of Flii and its interactome (*SI Appendix*, Fig. S9). It is possible that this region of the GLD is required for TMOD1 or LMOD2 interaction and the preferential localization of Flii to the M-line, and that these interactions in this location are critical in driving the function of Flii in effecting thin filament length. However, it is mysterious why the loss of these interactions with the R1245H mutant protein now targets Flii more exclusively to the Z-line, where the WT protein is only minorly observed. In summary, this study is the first to identify and model a novel human genetic variant as contributing to cardiomyopathy and it

adds to an ever-expanding list of genetic determinants underlying human heart disease.

Materials and Methods

A full description of the *Materials and Methods* is provided in the *SI Appendix*, such as description of animal use, generation or the various transgenic and gene targeted mouse models, animal surgeries, western blotting, immunohistochemistry, electron microscopy, adeno-associated virus use, and biochemical and in vitro assays.

Data, Materials, and Software Availability. All study data are included in the article and/or *SI Appendix*. In addition, the raw cardiac mass spectrometry data will be made fully available upon request as an Excel spreadsheet, and no other data are outstanding that are related to this study. The materials consisting of genetically altered mice for Flii expression, recombinant viruses and plasmids for Flii, or recombinant Flii protein will be available upon request and after completing a material transfer agreement.

ACKNOWLEDGMENTS. We would like to thank Dr. Christopher Newton-Cheh (Mass General Hospital, Harvard) for initial help in interrogating previous human GWAS data sets in the public domain. This work was supported by grants from NIH, National Heart, Lung and Blood Institute to J.D.M. (R01HL060562 and R01HL132831) and to J.P.P. (K08HL159346).

Author affiliations: [a]Department of Pediatrics, Cincinnati Children's Hospital Medical Center, Cincinnati, OH 45229; [b]Division of Cardiology, University of California San Francisco, San Francisco, CA 94158; and [c]Department of Pediatrics, Cincinnati Children's Hospital and the University of Cincinnati, Cincinnati, OH 45229

1. B. Ziaeian, G. C. Fonarow, Epidemiology and aetiology of heart failure. *Nat. Rev. Cardiol.* **13**, 368–378 (2016).
2. E. M. McNally, D. Y. Barefield, M. J. Puckelwartz, The genetic landscape of cardiomyopathy and its role in heart failure. *Cell Metab.* **21**, 174–182 (2015).
3. M. K. Freund *et al.*, Phenotype-specific enrichment of mendelian disorder genes near GWAS regions across 62 complex traits. *Am. J. Hum. Genet.* **103**, 535–552 (2018).
4. C. Vasilescu *et al.*, Genetic basis of severe childhood-onset cardiomyopathies. *J. Am. Coll. Cardiol.* **72**, 2324–2338 (2018).
5. Z. N. Al-Hassnan *et al.*, Categorized genetic analysis in childhood-onset cardiomyopathy. *Circ. Genom. Precis. Med.* **13**, 504–514 (2020).
6. M. E. Montasser *et al.*, Genetic and functional evidence links a missense variant in B4GALT1 to lower LDL and fibrinogen. *Science* **374**, 1221–1227 (2021).
7. W. J. McKenna, D. P. Judge, Epidemiology of the inherited cardiomyopathies. *Nat. Rev. Cardiol.* **18**, 22–36 (2021).
8. K. Musunuru *et al.*, Genetic testing for inherited cardiovascular diseases: A scientific statement from the american heart association. *Circ. Genom. Precis. Med.* **13**, e000067 (2020).
9. R. Yotti, C. E. Seidman, J. G. Seidman, Advances in the genetic basis and pathogenesis of sarcomere cardiomyopathies. *Annu. Rev. Genomics Hum. Genet.* **20**, 129–153 (2019).
10. J. Davis *et al.*, A tension-based model distinguishes hypertrophic versus dilated cardiomyopathy. *Cell* **165**, 1147–1159 (2016).
11. L. Thierfelder *et al.*, Alpha-tropomyosin and cardiac troponin T mutations cause familial hypertrophic cardiomyopathy: A disease of the sarcomere. *Cell* **77**, 701–712 (1994).
12. E. Ehler, Actin-associated proteins and cardiomyopathy–the 'unknown' beyond troponin and tropomyosin. *Biophys. Rev.* **10**, 1121–1128 (2018).
13. J. Kolb *et al.*, Thin filament length in the cardiac sarcomere varies with sarcomere length but is independent of titin and nebulin. *J. Mol. Cell Cardiol.* **97**, 286–294 (2016).
14. T. Tsukada *et al.*, Identification of residues within tropomodulin-1 responsible for its localization at the pointed ends of the actin filaments in cardiac myocytes. *J. Biol. Chem.* **286**, 2194–2204 (2011).
15. S. Yamashiro, D. S. Gokhin, S. Kimura, R. B. Nowak, V. M. Fowler, Tropomodulins: Pointed-end capping proteins that regulate actin filament architecture in diverse cell types. *Cytoskeleton (Hoboken)* **69**, 337–370 (2012).
16. V. M. Fowler, R. Dominguez, Tropomodulins and leiomodins: Actin pointed end caps and nucleators in muscles. *Biophys. J.* **112**, 1742–1760 (2017).
17. R. Littlefield, A. Almenar-Queralt, V. M. Fowler, Actin dynamics at pointed ends regulates thin filament length in striated muscle. *Nat. Cell Biol.* **3**, 544–551 (2001).
18. M. A. Sussman *et al.*, Myofibril degeneration caused by tropomodulin overexpression leads to dilated cardiomyopathy in juvenile mice. *J. Clin. Invest.* **101**, 51–61 (1998).
19. T. Tsukada *et al.*, Leiomodin-2 is an antagonist of tropomodulin-1 at the pointed end of the thin filaments in cardiac muscle. *J. Cell Sci.* **123**, 3136–3145 (2010).
20. C. T. Pappas *et al.*, Knockout of Lmod2 results in shorter thin filaments followed by dilated cardiomyopathy and juvenile lethality. *Proc. Natl. Acad. Sci. U S A* **112**, 13573–13578 (2015).
21. W. Witke *et al.*, Hemostatic, inflammatory, and fibroblast responses are blunted in mice lacking gelsolin. *Cell* **81**, 41–51 (1995).
22. T. Koana, Y. Hotta, Isolation and characterization of flightless mutants in drosophila melanogaster. *J. Embryol. Exp. Morphol.* **45**, 123–143 (1978).
23. H. G. de Couet, K. S. Fong, A. G. Weeds, P. J. McLaughlin, G. L. Miklos, Molecular and mutational analysis of a gelsolin-family member encoded by the flightless I gene of drosophila melanogaster. *Genetics* **141**, 1049–1059 (1995).
24. H. D. Campbell *et al.*, The drosophila melanogaster flightless-I gene involved in gastrulation and muscle degeneration encodes gelsolin-like and leucine-rich repeat domains and is conserved in caenorhabditis elegans and humans. *Proc. Natl. Acad. Sci. U.S.A.* **90**, 11386–11390 (1993).
25. G. L. Gabor Miklos, H. G. De Couet, The mutations previously designated as flightless-I3, flightless-O2 and standby are members of the W-2 lethal complementation group at the base of the X-chromosome of drosophila melanogaster. *J. Neurogenet.* **6**, 133–151 (1990).
26. D. Su *et al.*, The actin polymerization factor diaphanous and the actin severing protein flightless I collaborate to regulate sarcomere size. *Dev. Biol.* **469**, 12–25 (2021).
27. K. J. Karczewski *et al.*, The mutational constraint spectrum quantified from variation in 141,456 humans. *Nature* **581**, 434–443 (2020).
28. B. P. Prins *et al.*, Exome-chip meta-analysis identifies novel loci associated with cardiac conduction, including ADAMTS6. *Genome Biol.* **19**, 87 (2018).
29. S. H. Choi *et al.*, Rare coding variants associated with electrocardiographic intervals identify monogenic arrhythmia susceptibility genes: A multi-ancestry analysis. *Circ. Genom. Precis. Med.* **14**, e003300 (2021).
30. J. P. Pirruccello *et al.*, Analysis of cardiac magnetic resonance imaging in 36,000 individuals yields genetic insights into dilated cardiomyopathy. *Nat. Commun.* **11**, 2254 (2020).
31. J. P. Pirruccello *et al.*, Genetic analysis of right heart structure and function in 40,000 people. *Nat. Genet.* **54**, 792–803 (2022).
32. C. Roselli *et al.*, Multi-ethnic genome-wide association study for atrial fibrillation. *Nat. Genet.* **50**, 1225–1233 (2018).
33. S. Shah *et al.*, Genome-wide association and mendelian randomisation analysis provide insights into the pathogenesis of heart failure. *Nat. Commun.* **11**, 163 (2020).
34. I. Mohammad *et al.*, Flightless I is a focal adhesion-associated actin-capping protein that regulates cell migration. *FASEB J.* **26**, 3260–3272 (2012).
35. Y. T. Liu, H. L. Yin, Identification of the binding partners for flightless I, A novel protein bridging the leucine-rich repeat and the gelsolin superfamilies. *J. Biol. Chem.* **273**, 7920–7927 (1998).
36. X. L. Strudwick, A. J. Cowin, Multifunctional roles of the actin-binding protein flightless I in inflammation, cancer and wound healing. *Front. Cell Dev. Biol.* **8**, 603508 (2020).
37. H. D. Campbell *et al.*, Fliih, a gelsolin-related cytoskeletal regulator essential for early mammalian embryonic development. *Mol. Cell Biol.* **22**, 3518–3526 (2002).
38. J. Davis, M. Maillet, J. M. Miano, J. D. Molkentin, Lost in transgenesis. *Circ. Res.* **111**, 761–777 (2012).
39. E. M. Blanchard *et al.*, Targeted ablation of the murine α-tropomyosin gene. *Circ. Res.* **81**, 1005–1010 (1997).
40. S. P. Harris *et al.*, Hypertrophic cardiomyopathy in cardiac myosin binding protein-C knockout mice. *Circ. Res.* **90**, 594–601 (2002).
41. K. T. Bliss *et al.*, Phosphorylation of tropomodulin1 contributes to the regulation of actin filament architecture in cardiac muscle. *FASEB J.* **28**, 3987–3995 (2014).
42. Z. Kopecki, R. Arkell, B. C. Powell, A. J. Cowin, Flightless I regulates hemidesmosome formation and integrin-mediated cellular adhesion and migration during wound repair. *J. Invest. Dermatol.* **129**, 2031–2045 (2009).
43. H. Marei *et al.*, Differential Rac1 signalling by guanine nucleotide exchange factors implicates FLII in regulating Rac1-driven cell migration. *Nat. Commun.* **7**, 10664 (2016).
44. L. Mi-Mi *et al.*, In vivo elongation of thin filaments results in heart failure. *PLoS One* **15**, e0226138 (2020).
45. A. J. Cowin, N. Hatzirodos, J. T. Teusner, D. A. Belford, Differential effect of wounding on actin and its associated proteins, paxillin and gelsolin, in fetal skin explants. *J. Invest. Dermatol.* **120**, 1118–1129 (2003).